Journal of Biomechanics 47 (2014) 1045–1051

Contents lists available at ScienceDirect

Journal of Biomechanics

journal homepage: www.elsevier.com/locate/jbiomech
www.JBiomech.com

Patellar mechanics during simulated kneeling in the natural and implanted knee

Tariq R. Abo-Alhol [a], Clare K. Fitzpatrick [a], Chadd W. Clary [a], Adam J. Cyr [b], Lorin P. Maletsky [b], Peter J. Laz [a], Paul J. Rullkoetter [a,*]

[a] Center for Orthopaedic Biomechanics, University of Denver, 2390 S. York St., Denver, CO 80208, USA
[b] Experimental Joint Biomechanics Laboratory, University of Kansas, Lawrence, KS, USA

ARTICLE INFO

Article history:
Accepted 22 December 2013

Keywords:
Kneeling
Bone strain
Patella
Total knee replacement

ABSTRACT

Kneeling is required during daily living for many patients after total knee replacement (TKR), yet many patients have reported that they cannot kneel due to pain, or avoid kneeling due to discomfort, which critically impacts quality of life and perceived success of the TKR procedure. The objective of this study was to evaluate the effect of component design on patellofemoral (PF) mechanics during a kneeling activity. A computational model to predict natural and implanted PF kinematics and bone strains after kneeling was developed and kinematics were validated with experimental cadaveric studies. PF joint kinematics and patellar bone strains were compared for implants with dome, medialized dome, and anatomic components. Due to the less conforming nature of the designs, change in sagittal plane tilt as a result of kneeling at 90° knee flexion was approximately twice as large for the medialized-dome and dome implants as the natural case or anatomic implant, which may result in additional stretching of the quadriceps. All implanted cases resulted in substantial increases in bone strains compared with the natural knee, but increased strains in different regions. The anatomic patella demonstrated increased strains inferiorly, while the dome and medialized dome showed increases centrally. An understanding of the effect of implant design on patellar mechanics during kneeling may ultimately provide guidance to component designs that reduces the likelihood of knee pain and patellar fracture during kneeling.

1. Introduction

Kneeling after total knee replacement (TKR) has frequently been cited as a limiting activity for patients (Weiss et al., 2002; Noble et al., 2005). Many patients have reported that they cannot kneel due to pain, or avoid kneeling due to discomfort (Shafi et al., 2005; Hassaballa et al., 2002; Nijs et al., 2006; Palmer et al., 2002). For many TKR patients, kneeling is of particular cultural relevance, or is a requirement of their daily activities (praying, gardening). As a result, the ability or lack of ability to kneel without discomfort critically impacts quality of life and perceived success of the TKR procedure (Weiss et al., 2002).

While there are a variety of potential sources of knee pain during kneeling, including scar position (Nijs et al., 2006; Schai et al., 1999), the patellar bone contains numerous pain-sensing mechanoreceptors (Wojtys et al., 1990, McDougall, 2006), and is a likely contributor to anterior knee pain. During kneeling, the ground reaction force on the tibial tuberosity and/or patella causes a posteriorly-directed shear force on the tibia and compressive force on the patella (Incavo et al., 2004; Goldstein et al., 2007). After TKR, patellofemoral conformity, patellar tracking and strains are significantly altered from the native joint. Prior TKR studies have reported bone strains in resected patellae which are substantially higher than the natural knee (McLain and Barger, 1986; Reuben et al., 1991; Lie et al., 2005; Wulff and Incavo, 2000; Fitzpatrick et al., 2011), with resected patellae being more vulnerable to fracture due to sagittal plane bending in deep flexion, particularly in thinner patellae (Reuben et al., 1991). A high flexion, high patellofemoral (PF) contact force activity, such as kneeling, suggests that patients kneeling after TKR may be particularly susceptible to anterior knee pain and patellar fracture (Windsor et al., 1989).

A number of clinical studies have attributed PF complications, including patellar fracture and patellar bone strain, to prosthesis design (Brick and Scott, 1988; Healy et al., 1995; Theiss et al., 1996; Meding et al., 2008; McLain and Barger, 1986). Studies which have investigated the biomechanics of kneeling in TKR knee have predominantly focused on tibiofemoral (TF) kinematics, evaluating in vivo six-degree-of-freedom (6-DOF) kinematics through radiographic techniques (Hanson et al., 2007; Hamai et al., 2008; Incavo et al., 2004; Kanekasu et al., 2004; Coughlin et al., 2007). A number of cadaveric studies have utilized pressure-sensitive

* Corresponding author. Tel.: +1 303 871 3512; fax: +1 303 871 4450.
E-mail address: prullkoe@du.edu (P.J. Rullkoetter).

0021-9290/$ - see front matter © 2014 Elsevier Ltd. All rights reserved.
http://dx.doi.org/10.1016/j.jbiomech.2013.12.040

film to measure PF or TF contact area and pressure in response to kneeling, employing a compressive force, in addition to a quadriceps load, in order to simulate the loads encountered during kneeling (Wilkens et al., 2007; Hofer et al., 2011). Other in vitro studies have measured patellar bone strain using strain gauges attached to the anterior surface of the patella, but have not performed these analyses during a kneeling activity (McLain and Barger, 1986; Wulff and Incavo, 2000; Lie et al., 2005; Reuben et al., 1991). Computational methods have been used to develop high flexion models which have been applied to predict ligament and joint forces but have not been utilized to evaluate knee mechanics under loading conditions which simulate kneeling (Yang et al., 2010; Zelle et al., 2011), or to compare component designs under the high flexion, high PF force loading conditions representative of a kneeling activity.

The objective of the current study was to evaluate the effect of component design on patellar mechanics during a kneeling activity. A computational model to predict PF kinematics and strains after kneeling was developed and kinematics were validated against experimental cadaveric studies. A series of computational models, which included representations of both the native joint and a variety of TKR designs were compared during a simulated kneeling activity. PF joint kinematics and patellar bone strains were compared across multiple specimen-specific finite element (FE) models. An understanding of the effect of implant design on patellar mechanics during kneeling may ultimately provide guidance to component design that reduces the likelihood of knee pain and patellar fracture during kneeling.

2. Materials and methods

2.1. In-vitro cadaveric testing

A series of in vitro tests, designed to simulate a kneeling activity, were performed on four cadaveric knee specimens (male; age: 61.8 ± 13.8 years; height: 1.76 ± 0.08 m; weight: 76.67 ± kg). Each test was initially conducted on the natural knee, with the skin, joint capsule, knee ligaments and musculature intact. Subsequently, testing was performed on a posterior-stabilized (PS) TKR knee system, implanted by an orthopedic surgeon, with two distinct styles of patellar component, a 3 mm medialized dome and an anatomic design, with a consistent femoral and tibial geometry.

The femoral and tibial bone of each specimen was transected approximately 20 cm from the joint line, cemented into aluminum fixtures and mounted in a quasi-static knee rig (QKR) which permitted loading of the quadriceps and contact with a floor to simulate kneeling (Fig. 1). An aluminum clamp was used to rigidly attach the rectus femoris (RF) and vastus intermedius (VI) tendons such that they were actuated along the line-of-action of the femoral shaft. Superior–inferior (S–I) and anterior–posterior (A–P) translation of the simulated ankle position was constrained, while other degrees-of-freedom (DOF) were unconstrained. Knee flexion was achieved through S–I and A–P motion of the simulated hip. The knee was flexed to 90° TF flexion, while maintaining a vertical femur, until the patella made contact with the floor, which was represented by a metal plate with adjustable height. A 90 N load was applied to the quadriceps through free weights attached to the quadriceps tendon, while a contact force of 180 N between the patella and the floor was applied as a result of the weight of the fixtures and femur. The 90 N quadriceps loading counterbalances the weight of the hip sled in the experimental rig and allows the knee flexion angle to remain static.

An Optotrak 3020 (Northern Digital, Waterloo, Ontario) motion analysis system was used to track 6-DOF kinematics of the femur, tibia and patella bones throughout the activity through light emitting diode markers which were rigidly fixed to each bone. A hand-held digitizer was used to collect location data on each TKR component and bone surface relative to its respective local coordinate frame in order to determine component alignment relative to the bone. Magnetic resonance (MR) images (slice thickness of 1 mm; in-plane resolution of 0.234 × 0.234) were obtained for each specimen prior to implantation.

2.2. Finite element model development and kinematic validation

Specimen-specific FE models, which reproduced the in vitro experiment, were developed in Abaqus/Explicit (SIMULIA, Providence, RI) and based on previous models validated for kinematic prediction (Baldwin et al., 2009). Geometry of femoral, tibial and patellar bone and cartilage were segmented from the MR scans using ScanIP software (Simpleware, Exeter, UK). Size-matched TKR component geometry was generated from computer-aided-design surfaces obtained from the manufacturer. Bones and the femoral component were meshed with rigid triangular shell elements, and tibial and patellar components and all articular cartilage surfaces were meshed with deformable, eight-noded hexahedral elements. Implant components were positioned under the guidance of an orthopedic surgeon. The dome was positioned as medial and superior as possible while avoiding overhang. Implanted models also included a layer of bone cement between the patellar component and bone which was meshed with hexahedral elements. For the kinematic validation analyses, bone and the femoral component were modeled as rigid for computational efficiency. Tibial and patellar components were modeled as a nonlinear elastic–plastic material (Halloran et al., 2005a, 2005b), while linear material models were used for bone cement (E=3400 MPa, ν=0.3) and femoral, tibial and patellar articular cartilage (E=12 MPa, ν=0.45). A coefficient of friction of 0.04 was applied between metal–polyethylene articulating surfaces (Halloran et al., 2005a, 2005b). The patellar tendon, RF and vasti tendons were represented by deformable hyperelastic membrane elements with fiber-reinforcement, with uniaxial tension characteristics calibrated to match published experimental measurements (Atkinson et al., 1997; Stäubli et al., 1999). The vasti tendon was separated into five bundles representing the VI, vastus lateralis longus (VLL), vastus lateralis obliquus (VLO), vastus medialis longus (VML) and vastus medialis obliquus (VMO) (Fitzpatrick et al., 2011). Contact was defined between all soft-tissue structures and relevant bone and articular surfaces to allow wrapping in deep flexion. In order to directly reproduce the experimental setup, loading in this case was only applied to the VI bundle of the vasti tendon.

The model was first aligned in the initial position of the kneeling activity based on the measured positions obtained during cadaveric testing. During the kneeling simulation, TF kinematics were fully prescribed based on the experimentally measured kinematics. The patella was kinematically unconstrained, with a 90 N load applied to the RF and VI bundles of the quadriceps, and a compressive load matching the experimental loading condition (180 N) applied to the patella via contact with the floor. 6-DOF PF kinematics were measured in the same manner as the experiment, and compared to the in vitro data.

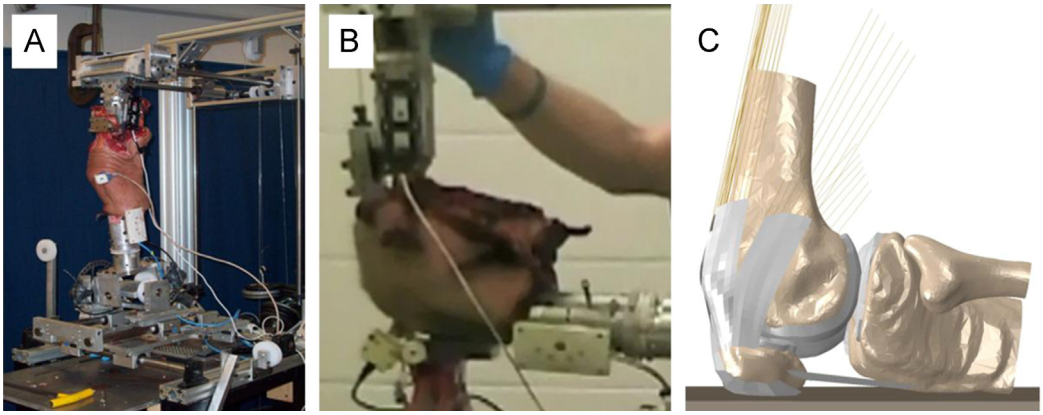

Fig. 1. (A) Knee specimen fixed in the quasi-static knee rig; (B) experimental kneeling simulation in the quasi-static knee rig; and (C) computational simulation of the kneeling experiment.

2.3. Application and strain predictions for multiple patellae

Utilizing the computational model described above, the boundary conditions were adapted to better represent the physiological loads applied during kneeling which were not feasible to implement experimentally (including higher contact load and quadriceps load, with quadriceps load distributed throughout all vasti bundles). Models were developed for an additional set of eight specimens (male; age: 67 ± 10 years; height: 1.78 ± 0.05 m; weight: 83 ± 14 kg). In addition to MR images, computed tomography (CT) images were obtained for each specimen. The CT scans were used to develop specimen-specific models of the patellar bone with distributed material properties in order to evaluate strain in the patellar bone. Patellar bone was meshed with hexahedral elements with material properties developed from the CT data using BoneMat (Taddei et al., 2007). A linear relationship adopted from the literature (Peng et al., 2006) was used to correlate Hounsfield units (HU) to apparent density (ρ). The empirical relationship, Young's Modulus (E)$=1990\rho^{3.46}$, was applied to convert bone density to mechanical properties (Keller, 1994). A convergence study was performed on a single specimen to determine the optimal element size for the patellar bone mesh. Meshes were generated with average element edge lengths of 1.5, 1.25, 1.0, 0.8 and 0.5 mm. Strain prediction converged with a patellar bone element edge length of 1.0 mm, with the finer meshes showing differences of less than 3% in predicted highly strained volume, and this was subsequently used on all models.

The knee was again placed in a 90° TF kneeling position, while the PF joint remained unconstrained. A muscle load of 550 N was distributed among the quadriceps bundles according to their physiological cross-sectional area (Farahmand et al., 1998), while a compressive load of 330 N ($\frac{1}{2}$ BW, representing double-stance kneeling) was applied through the floor.

In addition to the natural knee and two TKR knees evaluated previously, a third TKR design with a dome-compatible patellar component was also evaluated in this computational setup.

Patellar bone strain (as a surrogate measure for likelihood of anterior knee pain and fracture) was predicted from the FE models and compared between natural and implanted conditions, and also compared between regions (superior, inferior, medial and lateral quadrants) of the patellar bone. A highly strained bone volume was used to compare changes in bone strain between conditions (Fitzpatrick et al., 2011). The highly strained bone volume, representing the bone volume experiencing strain above a specific threshold level, is likely a better predictor of bone failure than a peak strain value, which may occur in a small localized region and can be highly dependant on mesh construction. A threshold of 0.5% (just below reported bone yield strain) was applied in the current analysis. In addition to bone strain, PF contact pressure and area were compared between analyses.

3. Results

Comparing PF kinematics between the experiment and the computational model, maximum differences in PF translations and rotations were 1.1 mm and 1°, respectively, across all four specimens in both the natural and implanted conditions (Fig. 2). Root mean square differences were less than 0.65 mm and 0.5° for translations and rotations, respectively (Table 1). Prior to kneeling, sagittal plane patellar tilt was significantly greater in all implanted conditions than the natural case (tilt of $10.2 \pm 4.2°$, $20.6 \pm 5.2°$, $24.4 \pm 4.5°$ and $25.3 \pm 3.9°$ for natural, anatomic, medialized-dome and dome, respectively). After contact with the floor, sagittal plane patellar tilt was reduced to $7.9 \pm 2.6°$, $18.5 \pm 5.2°$, $19.5 \pm 3.7°$, $19.6 \pm 3.6°$ for natural, anatomic, medialized-dome and dome conditions, respectively. Due to the less conforming nature of the designs, change in sagittal plane tilt as a result of kneeling was larger for the medialized-dome and dome implants than the natural case or anatomic implant (Fig. 3). This resulted in more inferior contact on the anterior surface of the patella against the floor for the natural and anatomic designs, compared to the medialized-dome and dome designs.

As a result of the load on the patella, there was a considerable increase in both PF contact pressure and area before and after kneeling (Fig. 4). Due to the compression-dominated loading condition, minimum principal strains were on the order of 3 × larger than maximum principal strains, and are reported in the current study. Kneeling resulted in an average of 8.3%, 16.0%, 12.5% and 13.2% increase in highly strained bone volume in natural, anatomic, medialized dome and dome conditions, respectively.

Table 1
Average RMS differences between model and experimental patellofemoral kinematics during kneeling for all four specimens.

Kinematic output	Kinematic output average RMS difference ± standard deviation (deg)-mm		
	Natural	Anatomic	Medialized dome
Flexion	0.25 ± 0.07	0.29 ± 0.12	0.42 ± 0.13
Internal–external rotation	0.12 ± 0.01	0.12 ± 0.02	0.11 ± 0.02
Spin	0.19 ± 0.03	0.10 ± 0.02	0.21 ± 0.06
Anterior–posterior translation	0.27 ± 0.08	0.08 ± 0.01	0.35 ± 0.14
Medial–lateral shift	0.14 ± 0.02	0.12 ± 0.02	0.15 ± 0.03
Superior–inferior translation	0.65 ± 0.47	0.05 ± 0.01	0.33 ± 0.12

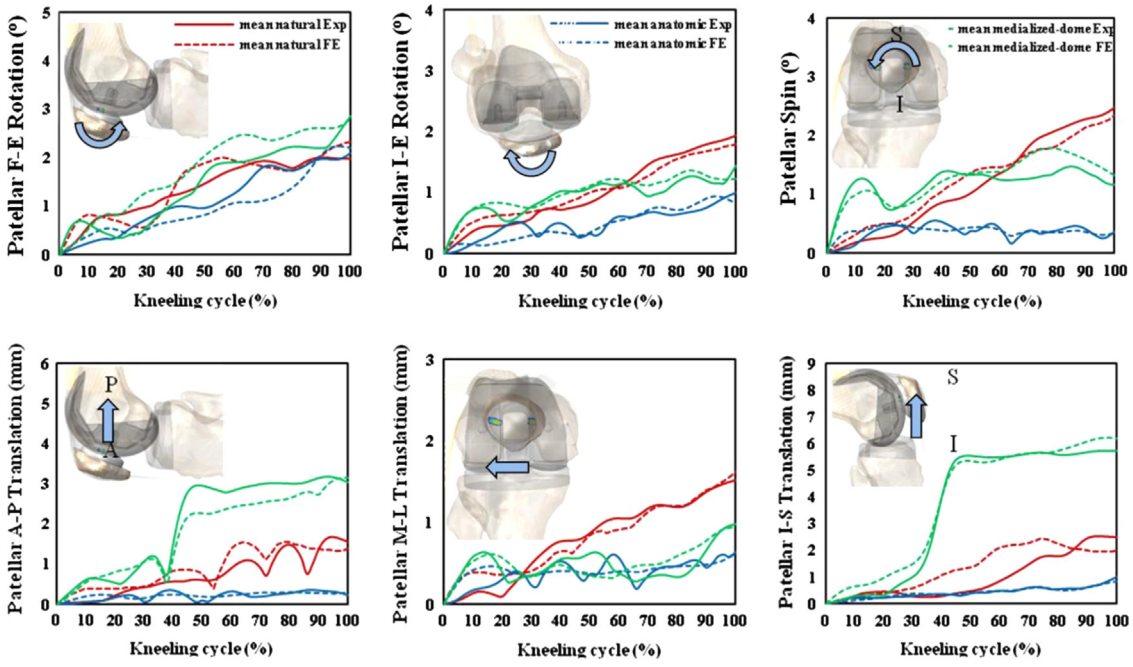

Fig. 2. Comparison between experimentally-measured and FE model predicted PF kinematics during kneeling for the natural knee, modified dome and anatomic patellar components. Shown for the average of all four specimens.

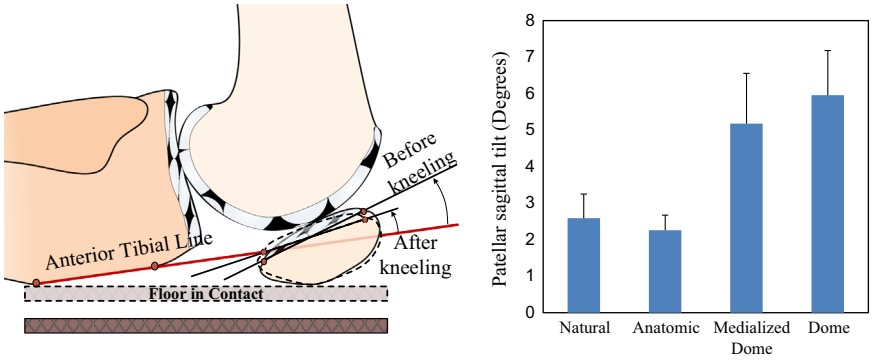

Fig. 3. Measurement of sagittal plane patellar tilt, and representation of the typical change (reduction) in tilt as a result of kneeling (left); average change (and standard deviation) in sagittal plane tilt for natural and TKR knees as a result of kneeling (right).

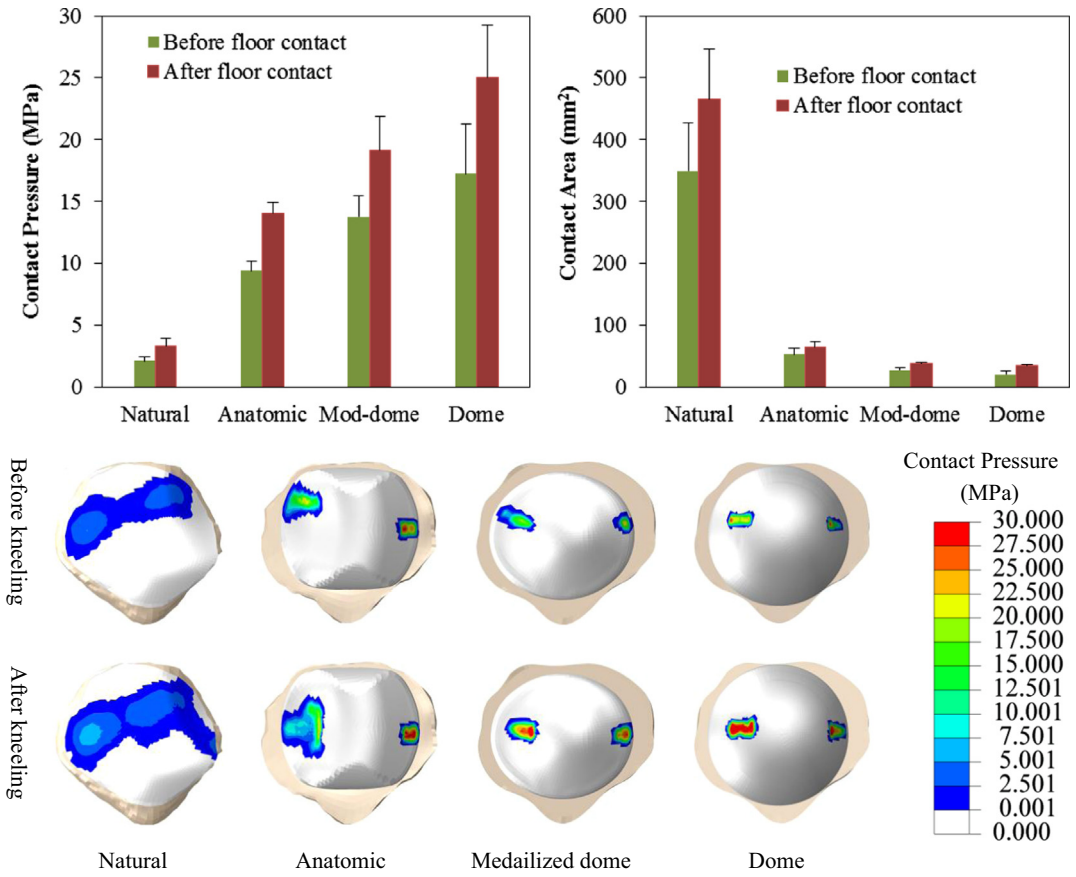

Fig. 4. Mean and standard deviations in peak contact pressure and contact area before and after kneeling for natural and TKR conditions (top); contact pressure for a representative subject before and after kneeling (bottom).

Of the three TKR assessed, the medialized dome demonstrated the lowest bone strain, both before and after kneeling. Highly strained bone volumes were on average 2.3, 1.8, and 2.1 times higher than the natural case for anatomic, medialized dome and dome designs, respectively (Figs. 5 and 6).

Bone strain distribution after kneeling reflected the differences in patellar contact, and resulted in larger compressive strains centrally in the natural condition, and inferiorly, medially and laterally in the implanted cases. The medial and lateral quadrants experienced the largest highly strained bone volumes across all conditions; this increased significantly as a result of kneeling for all implanted conditions, but there was no significant change in the natural condition. Anatomic and dome components also experienced significant increase in bone strain in the inferior portion of the patellar bone (Table 2).

4. Discussion

Good agreement in PF kinematics between experimental measurements and computational predictions, and appropriate differentiation between conditions, highlight the applicability of the computational model as a complementary tool to experimental testing. As in this study, a limited number of experimental tests may be performed to provide adequate kinematic validation for the computational model, and the model can subsequently be employed to perform additional simulations or modifications to the boundary conditions that would not be practical experimentally. While it is not possible to provide experimental data to verify the internal bone strain predictions from this study, good agreement in kinematics provide confidence in the boundary conditions being applied in the model. There are several studies in the literature that have measured anterior surface strain on

the patella during cadaveric experiments. McLain and Barger (1986) found that anterior surface strain in the patella was increased up to three times that of natural controls. Reuben et al. (1991) evaluated natural and implanted anterior patellar surface strains using a variety of resection thicknesses and a quadriceps load of up to 600 N at 90°s flexion. They found significant increases in anterior patellar strain with resurfacing, with reported strains of over 2500 μ strain for an ideal thickness, and almost 3500 μ strain for a thin patellar resection. A similar study from Lie et al. (2005) found again a significant increase in strain with resurfacing, with strains up to 1000 μ strain on the anterior surface of the patella with a 500 N quad load at 90° flexion. Although these studies are limited to the location of the strain gage and measuring the tensile strains on the patellar surface, the magnitude is similar to that reported here, in addition to the substantial increase in strains with resurfacing.

For comparison purposes, the most related previous study (Fitzpatrick et al., 2011) has shown that the range of predicted strains is similar to that reached during the deep flexion position during a squat. Using the same measures, the maximum flexion position during squat averaged a 10% highly strained volume, with some specimens over 20%. In the current study, kneeling resulted in an average over 15% highly strained volume for the three implant types evaluated, with one over 20%. This could be an indication of why kneeling is avoided by some patients due to pain.

The largest difference between patellar designs was bone strain in the inferior portion of the patella between anatomic components and medialized-dome and dome components. The anatomic patella, with sagittal plane tilt closest to the natural condition prior to kneeling, has the greatest amount of congruency between femoral and patellar components. As a result of this geometric constraint, the anatomic component experienced the smallest reduction in sagittal plane tilt and consequently the anterior surface of the patella experienced more inferior contact with the floor, increasing the bending moment and bone strain near the distal pole of the patella. This result is supported by prior clinical

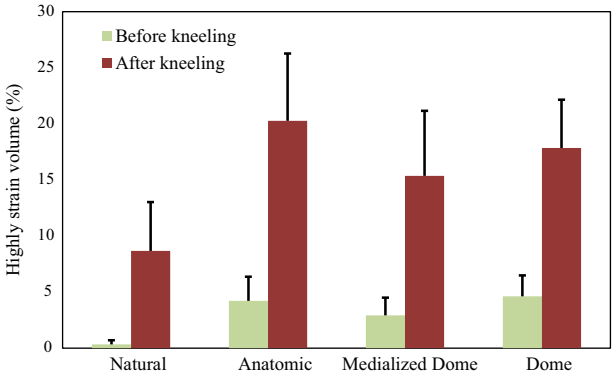

Fig. 5. Mean and standard deviation in highly strained bone volume before and after kneeling for natural knee and TKR implants.

Table 2
Highly strained bone volume before and after kneeling (%).

	Inferior	Superior	Medial	Lateral
Natural	0.0–2.0	0.0–2.9	0.1–4.6	0.3–6.8
Anatomic	1.5–21.4	0.5–1.3	3.1–17.8	7.2–18.1
Medialized-dome	0.2–7.0	0.1–1.0	2.8–20.5	5.4–14.0
Dome	3.4–14.9	1.1–5.1	3.1–16.3	6.0–16.5

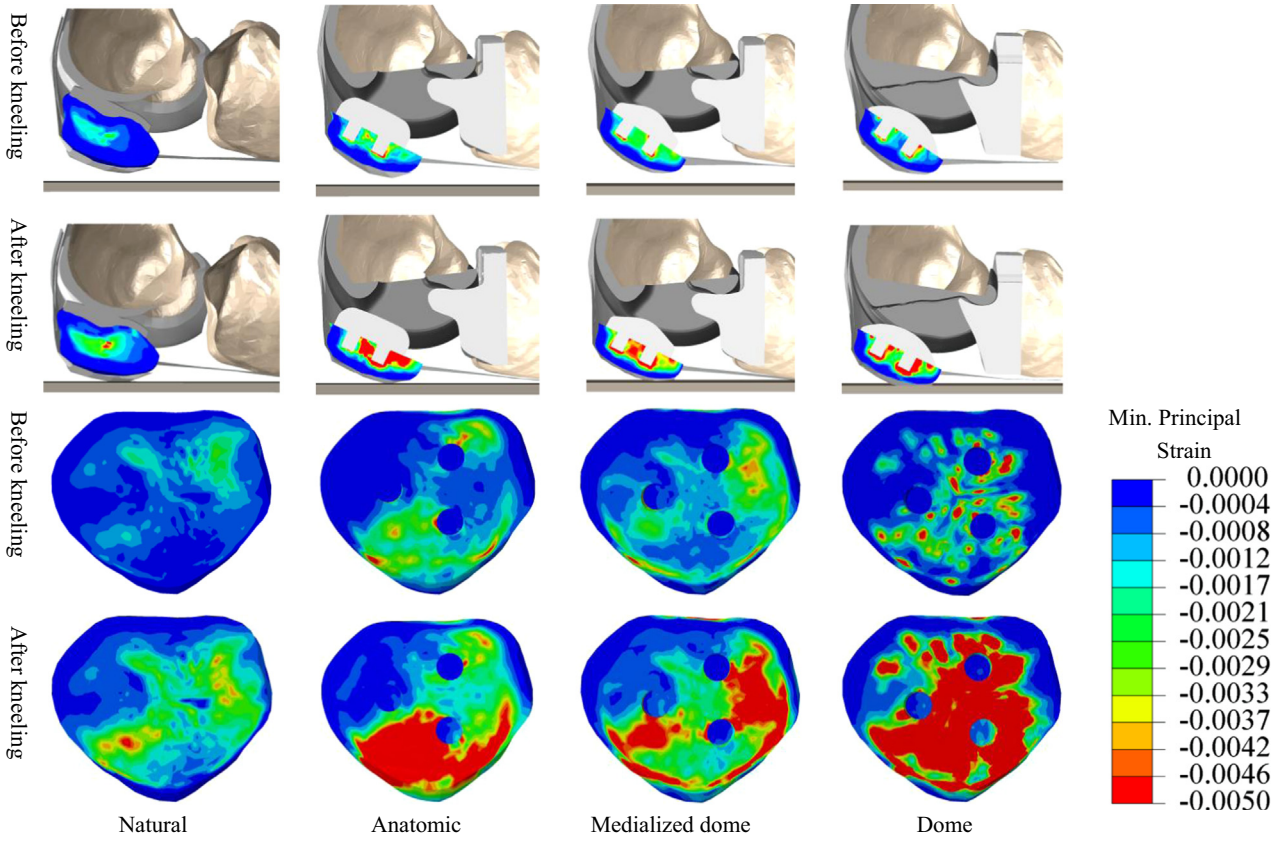

Fig. 6. Compressive bone strain before and after kneeling for natural knee and TKR implants, shown for a representative subject.

studies from MacCollum et al. (1989), which reported PF complications in a series of 87 TKR knees with anatomic patellar components. Five cases of patellar fracture were deemed to be caused by increased forces in the patella due the shape of the articulation. In our analysis, an increase in strain in the inferior region was not seen in medialized-dome and dome designs as the change in sagittal plane tilt was significantly higher than the anatomic design, moving the contact between the anterior patella and the floor more superior, which facilitated loading sharing of the compressive load between medial, lateral and inferior regions. While sagittal plane tilt for the dome was similar to the medialized dome design, the dome experienced higher bone strain as a result of higher contact pressure due to lack of congruency and smaller PF contact area.

The sagittal plane tilt that occurs with kneeling may stretch the extensor mechanism, quadriceps muscle or PF soft-tissues, another potential source of pain or limitation during kneeling, and it is therefore assumed that more natural behavior is desirable. The anatomic component was similar to the natural in this output, with the dome and medialized dome approximately twice the rotation.

There are a number of notable limitations to the current study. The study assessed a single style of kneeling – anterior force was predominately on the patella. Alternative kneeling conditions could result in shifting of floor contact from the patella to the tibial tubercle with greater flexion angles. These conditions and additional flexion angles warrant further investigation, and the kneeling model described in this study provides an appropriate platform for further comparative analyses. Variability in tibiofemoral kinematics would have some influence on the patellofemoral position during kneeling, although it is assumed that this is a relatively small effect. Although the kinematic predictions were validated against experimental data, strain predictions were not, primarily due to the difficulty of determining a strain distribution experimentally. Evaluating potential for knee pain during kneeling based on bone strain and sagittal plane tilt is obviously a simplification given the multi-factorial nature and complexity of pain responses. While there are a multitude of TKR designs available, we believe that the three designs evaluated in the current study are representative of the primary styles of patellar components (anatomic, medialized dome, dome) that are currently commercially available. This study has demonstrated the effect of and tradeoffs associated with selection of current patellar components, and as none of the current patellar styles have demonstrated that they are ultimately superior in terms of clinical performance (Schindler, 2012), highlighted criteria for design considerations in order to assist future patients with kneeling.

Conflict of interest statement

One of the authors (PJR) is a consultant to DePuy Synthes Inc.

Acknowledgments

This study was supported in part by DePuy Synthes, Inc.

References

Atkinson, T., Haut, R., Altiero, N., 1997. A poroelastic model that predicts some phenomenological responses of ligaments and tendons. J. Biomech. Eng. 119, 400.

Baldwin, M.A., Clary, C., Maletsky, L.P., Rullkoetter, P.J., 2009. Verification of predicted specimen-specific natural and implanted patellofemoral kinematics during simulated deep knee bend. J. Biomech. 42, 2341–2348.

Brick, G.W., Scott, R.D., 1988. The patellofemoral component of total knee arthroplasty. Clin. Orthop. Relat. Res. 231, 163–178.

Coughlin, K.M., Incavo, S.J., Doohen, R.R., Gamada, K., Banks, S., Beynnon, B.D., 2007. Kneeling kinematics after total knee arthroplasty: anterior–posterior contact position of a standard and a high-flex tibial insert design. J. Arthroplast. 22, 160–165.

Farahmand, F., Sejiavongse, W., Amis, A.A., 1998. Quantitative study of the quadriceps muscles and trochlear groove geometry related to instability of the patellofemoral joint. J. Orthop. Res. 16, 136–143.

Fitzpatrick, C.K., Baldwin, M.A., Ali, A.A., Laz, P.J., Rullkoetter, P.J., 2011. Comparison of patellar bone strain in the natural and implanted knee during simulated deep flexion. J. Orthop. Res. 29, 232–239.

Goldstein, W.M., Gordon, A.C., Branson, J.J., Simmons, C., Berland, K.A., 2007. Stress over the anterior aspect of the knee with kneeling. J. Bone Jt. Surg. 89, 162–166.

Halloran, J.P., Easley, S.K., Petrella, A.J., Rullkoetter, P.J., 2005b. Comparison of deformable and elastic foundation finite element simulations for predicting knee replacement mechanics. J. Biomech. Eng. 127, 813–818.

Halloran, J.P., Petrella, A.J., Rullkoetter, P.J., 2005a. Explicit finite element modeling of total knee replacement mechanics. J. Biomech. 38, 323–331.

Hamai, S., Miura, H., Higaki, H., Matsuda, S., Shimoto, T., Sasaki, K., Yoshizumi, M., Okazaki, K., Tsukamoto, N., Iwamoto, Y., 2008. Kinematic analysis of kneeling in cruciate-retaining and posterior-stabilized total knee arthroplasties. J. Orthop. Res. 26, 435–442.

Hanson, G.R., Park, S.E., Suggs, J.F., Moynihan, A.L., Nha, K.W., Freiberg, A.A., Li, G., 2007. In vivo kneeling biomechanics after posterior stabilized total knee arthroplasty. J. Orthop. Sci. 12, 476–483.

Hassaballa, M., Vale, T., Weeg, N., Hardy, J.R., 2002. Kneeling requirements and arthroplasty surgery. The Knee 9, 317–319.

Healy, W.L., Wasilewski, S.A., Takei, R., Oberlander, M., 1995. Patellofemoral complications following total knee arthroplasty: correlation with implant design and patient risk factors. J. Arthroplast. 10, 197–201.

Hofer, J.K., Gejo, R., McGarry, M.H., Lee, T.Q., 2011. Effects on tibiofemoral biomechanics from kneeling. Clin. Biomech. 26, 605–611.

Incavo, S.J., Mullins, E.R., Coughlin, K.M., Banks, S., Banks, A., Beynnon, B.D., 2004. Tibiofemoral kinematic analysis of kneeling after total knee arthroplasty. J. Arthroplast. 19, 906–910.

Kanekasu, K., Banks, S.A., Honjo, S., Nakata, O., Kato, H., 2004. Fluoroscopic analysis of knee arthroplasty kinematics during deep flexion kneeling. J. Arthroplast. 19, 998–1003.

Keller, T.S., 1994. Predicting the compressive mechanical behavior of bone. J. Biomech. 27, 1159–1168.

Lie, D., Gloria, N., Amis, A., Lee, B., Yeo, S., Chou, S., 2005. Patellar resection during total knee arthroplasty: effect on bone strain and fracture risk. Knee Surg. Sports Traumatol. Arthrosc. 13, 203–208.

MacCollum, M.S., Karpman, R.R., 1989. Complications of the PCA anatomic patella. Orthopedics 12, 1423–1428.

McDougall, J.J., 2006. Arthritis and pain: neurogenic origin of joint pain. Arthr. Res. Ther. 8, 220.

McLain, R.F., Barger, W.F., 1986. The effect of total knee design on patellar strain. J. Arthrop. 1, 91–98.

Meding, J.B., Fish, M.D., Berend, M.E., Ritter, M.A., 2008. Predicting patellar failure after total knee arthroplasty. Clin. Orthop. Relat. Res. 466, 2769–2774.

Nijs, J., Van Geel, C., Van de Velde, B., 2006. Diagnostic value of five clinical tests in patellofemoral pain syndrome. Man. Ther. 11, 69–77.

Noble, P.C., Gordon, M.J., Weiss, J.M., Reddix, R.N., Conditt, M.A., Mathis, K.B., 2005. Does total knee replacement restore normal knee function? Clin. Orthop. Relat. Res. 431, 157–165.

Palmer, S., Servant, C., Maguire, J., Parish, E., Cross, M., 2002. Ability to kneel after total knee replacement. J. Bone Jt. Surg. Br. Vol. 84, 220–222.

Peng, L., Bai, J., Zeng, X., Zhou, Y., 2006. Comparison of isotropic and orthotropic material property assignments on femoral finite element models under two loading conditions. Med. Eng. Phys. 28, 227–233.

Reuben, J.D., McDonald, C.L., Woodard, P.L., Hennington, L.J., 1991. Effect of patella thickness on patella strain following total knee arthroplasty. J. Arthroplast. 6, 251–258.

Schai, P., Gibbon, A., Scott, R., 1999. Kneeling ability after total knee arthroplasty: perception and reality. Clin. Orthop. Relat. Res. 367, 195–200.

Schindler, O.S., 2012. Basic kinematics and biomechanics of the patellofemoral joint. Part 2: The patella in total knee arthroplasty. Acta Orthop. Belg. 78, 11.

Shafi, M., Kim, Y.Y., Lee, Y.S., Kim, J.Y., Han, C.W., 2005. Patellar polyethylene peg fracture: a case report and review of the literature. Knee Surg. Sports Traumatol. Arthrosc. 13, 472–475.

Stäubli, H.U., Schatzmann, L., Brunner, P., Rincón, L., Nolte, L.-P., 1999. Mechanical tensile properties of the quadriceps tendon and patellar ligament in young adults. Am. J. Sports Med. 27, 27–34.

Taddei, F., Schileo, E., Helgason, B., Cristofolini, L., Viceconti, M., 2007. The material mapping strategy influences the accuracy of CT-based finite element models of bones: an evaluation against experimental measurements. Med. Eng. Phys. 29, 973–979.

Theiss, S.M., Kitziger, K.J., Lotke, P.S., Lotke, P.A., 1996. Component design affecting patellofemoral complications after total knee arthroplasty. Clin. Orthop. Relat. Res. 326, 183–187.

Weiss, J.M., Noble, P.C., Conditt, M.A., Kohl, H.W., Roberts, S., Cook, K.F., Gordon, M.J., Mathis, K.B., 2002. What functional activities are important to patients with knee replacements? Clin. Orthop. Relat. Res. 404, 172–188.

Wilkens, K.J., Duong, L.V., McGarry, M.H., Kim, W.C., Lee, T.Q., 2007. Biomechanical effects of kneeling after total knee arthroplasty. J. Bone Jt. Surg. 89, 2745–2751.

Windsor, R.E., Scuderi, G.R., Insall, J.N., 1989. Patellar fractures in total knee arthroplasty. J. Arthropl. 4, S63–S67.
Wojtys, E.M., Beaman, D.N., Glover, R.A., Janda, D., 1990. Innervation of the human knee joint by substance-P fibers. Arthroscopy 6, 254–263.
Wulff, W., Incavo, S.J., 2000. The effect of patella preparation for total knee arthroplasty on patellar strain. J. Arthroplast. 15, 778–782.
Yang, Z., Wickwire, A.C., Debski, R.E., 2010. Development of a subject-specific model to predict the forces in the knee ligaments at high flexion angles. Med. Biol. Eng. Comput. 48, 1077–1085.
Zelle, J., Janssen, D., Van Eijden, J., De Waal Malefijt, M., Verdonschot, N., 2011. Does high-flexion total knee arthroplasty promote early loosening of the femoral component? J. Orthop. Res. 29, 976–983.